VIP Supramolecular Chemistry Very Important Paper

How to cite: *Angew. Chem. Int. Ed.* **2023,** *62,* e202216475
International Edition: doi.org/10.1002/anie.202216475
German Edition: doi.org/10.1002/ange.202216475

Tailorable and Biocompatible Supramolecular-Based Hydrogels Featuring two Dynamic Covalent Chemistries

Ivana Marić, Liangliang Yang, Xiufeng Li, Guillermo Monreal Santiago, Charalampos G. Pappas, Xinkai Qiu, Joshua A. Dijksman, Kirill Mikhailov, Patrick van Rijn, and Sijbren Otto**

Abstract: Dynamic covalent chemistry (DCC) has proven to be a valuable tool in creating fascinating molecules, structures, and emergent properties in fully synthetic systems. Here we report a system that uses two dynamic covalent bonds in tandem, namely disulfides and hydrazones, for the formation of hydrogels containing biologically relevant ligands. The reversibility of disulfide bonds allows fiber formation upon oxidation of dithiol-peptide building block, while the reaction between NH–NH_2 functionalized C-terminus and aldehyde cross-linkers results in a gel. The same bond-forming reaction was exploited for the "decoration" of the supramolecular assemblies by cell-adhesion-promoting sequences (RGD and LDV). Fast triggered gelation, cytocompatibility and ability to "on-demand" chemically customize fibrillar scaffold offer potential for applying these systems as a bioactive platform for cell culture and tissue engineering.

[*] I. Marić, G. M. Santiago, C. G. Pappas, K. Mikhailov, S. Otto
Stratingh Institute, Centre for Systems Chemistry, University of Groningen
Nijenborgh 4, 9747 AG Groningen (The Netherlands)
E-mail: s.otto@rug.nl

I. Marić
Dutch Polymer Institute
P. O. Box 902, 5600 AX Eindhoven (The Netherlands)

L. Yang, P. van Rijn
University Medical Center Groningen, Department of Biomedical Engineering-FB40 and W. J. Kolff Institute for Biomedical Engineering and Materials Science-FB41, University of Groningen
A. Deusinglaan 1, 9713 AV Groningen (The Netherlands)
E-mail: p.van.rijn@umcg.nl

X. Li, J. A. Dijksman
Physical Chemistry and Soft Matter, Wageningen University
Stippeneng 4, 6708 WE Wageningen (The Netherlands)

X. Qiu
Stratingh Institute and Zernike Institute for Advanced Materials, University of Groningen
Nijenborgh 4, 9747 AG Groningen (The Netherlands)

Introduction

Currently, the field of materials science relies on a strategy that involves understanding and mimicking of structures and behaviors found in nature, to provide solutions in areas ranging from medicine and energy to environmental sustainability. In particular, synthetic biomaterials are being explored at a rapid pace, as they may have suitable properties to be used as extracellular matrices for tissue engineering.[1] Functional supramolecular polymers have been viewed as a powerful platform for such application since they are readily accessible from short peptides,[2] or peptide-amphiphiles,[3] containing binding sites for biologically functional ligands.[4] Cell adhesion motifs,[5] peptide sequences that can direct cell differentiation,[6] and susceptibility to degradation,[7] are important ingredients for successful 3D cell growth within synthetic materials.[8] Synthetic biomaterials show good batch-to-batch consistency, enabling the translation of basic research into clinical applications.[9,10]

DCC has the potential to provide synthetic materials with additional attractive features.[11] DCC has been recognized as a tool to study fundamental questions of living systems,[12] but also to access emergent behaviors of functional materials. For example, self-healing,[13] shape memory, and stimuli-induced stiffness changes can be achieved by implementing reversible bonds into dynamic hydrogels.[14] The combination of multiple orthogonal dynamic covalent chemistries[15] has made its way into functional materials only recently and has been used to enhance the responsiveness of polymer hydrogels through the use of doubly-labile crosslinkers.[13a,16a] In principle, the use of two reversible covalent linkages should allow these to be addressed separately, and used for different purposes, provided these linkages are orthogonal. In practice, this feature has yet to be exploited in hydrogel systems.

Here, we introduce a new peptide-based dynamic covalent hydrogel system that features two orthogonal reversible chemistries that fulfill three different roles: Dynamic disulfide bonds allow for self-templated synthesis of macrocycles that undergo supramolecular polymerization; Bioorthogonal dynamic hydrazone chemistry,[17] then allows for gelation through crosslinking of the resulting fibrous assemblies as well as their covalent functionalization with biologically relevant ligands. The resulting material has several attractive features for application in cell culture: Similar to the extracellular matrix (ECM), it possesses a

fibrous structure. Second, it allows the facile and on-demand attachment of biologically relevant ligands such as cell adhesion motifs (e.g., RGD, LDV),[5,18] or short peptide sequences known to direct differentiation of stem cells.[6,19] Third, due to its peptide nature, the material is likely to be cytocompatible.[20]

Results and Discussion

We used dynamic combinatorial chemistry previously to access fiber-like, supramolecular polymers from pseudo-peptide building blocks.[21] To improve the ability to tailor the resulting materials, we decided to introduce a second orthogonal reversible chemistry. Thus, we designed building block **1** (Scheme 1a) with three distinctive features: (i) a dithiol, aromatic core to promote thiol-disulfide exchange and stacking via π-π interactions; (ii) a short peptide chain that will assist self-assembly through β-sheet formation and is biocompatible;[9,20] and (iii) a hydrazide-functionalized C-terminus to enable further chemical reactivity through a second dynamic covalent bond.

Upon exposure to air, dithiol molecule **1** underwent oxidation to form a dynamic combinatorial library (DCL) of differently sized cyclic disulfides (dominated by $\mathbf{1}_3$, $\mathbf{1}_4$ and $\mathbf{1}_5$), which continuously interconvert by thiol-disulfide covalent exchange. In such a mixture, one of the rings (in this system $\mathbf{1}_5$) can form stacks with copies of itself, which promotes the process of self-assembly. This shifts the distribution of the exchange pool towards the synthesis of more of the self-assembling library member. Growth of the stacks from their ends, combined with breakage of stacks through mechanical agitation, increases the amount of supramolecular polymer (Scheme 1a, for the kinetic profile of $\mathbf{1}_5$ formation, see Figure S2a; for compositional analyses of the DCLs, see Figures S3–S13). Atomic force microscopy (AFM) and cryo transmission electron microscopy (cryo-TEM) of DCLs dominated by $\mathbf{1}_5$ (Figure S24) indicate the presence of fibers with lengths ranging from hundreds of nanometers to several micrometers.

Subsequently, we investigated the possibility of hydrogel formation upon addition of di- or trialdehydes (Scheme 1b) as crosslinkers. These crosslinkers differ in length and flexibility of the spacer groups between the aldehyde moieties, and the number of crosslinking groups (Scheme 1c). These were expected to induce different crosslinking arrangements within the gel network, potentially allowing the physical properties of the gels to be tuned. The concentration (4.0 mM in **1**) and the ratio of **1** to crosslinker (1:1 in complementary functionalities, i.e., NH–NH_2 and carbonyls) were kept constant in all experiments. Adding crosslinkers containing short and rigid spacers (**2**, **4**, **5**, and **7**) to the solutions of preformed fibers resulted in gel formation. Hydrogelation occurs in the span of 2 to 10 minutes, depending on the crosslinking reagent (Scheme 1d). In contrast, molecules with a flexible spacer **3**, **6**, and **8** yielded viscous solutions even upon prolonged incubation. We hypothesize that an increased distance

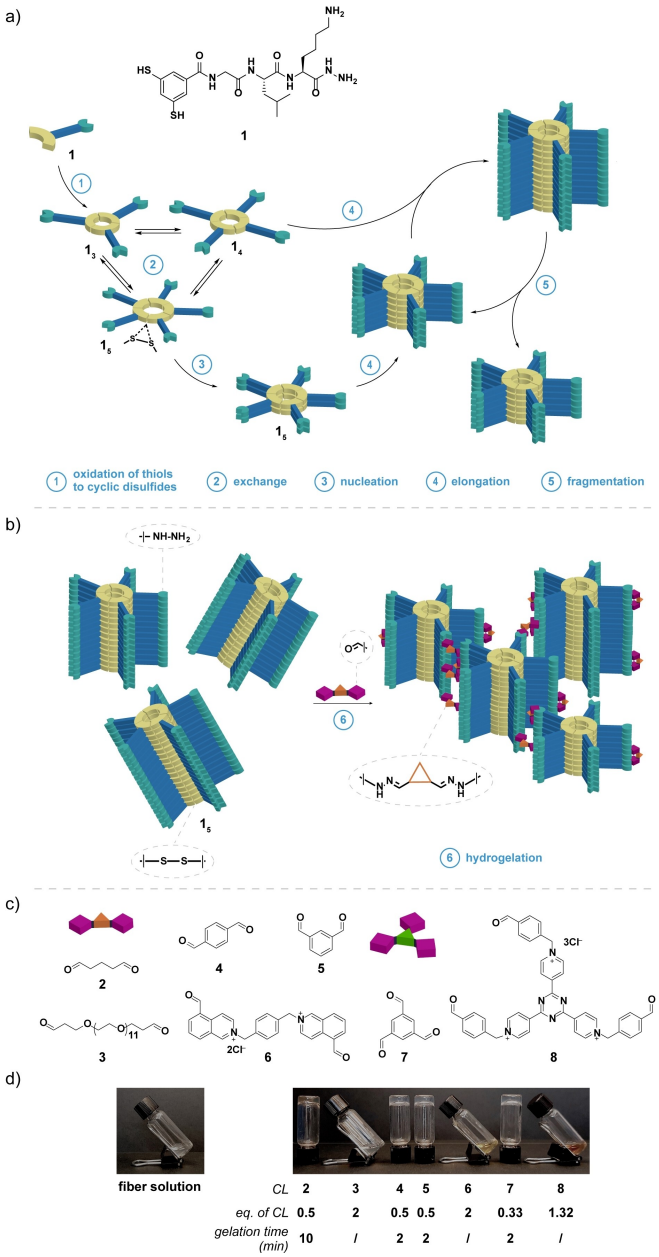

Scheme 1. a) Mechanism of fiber formation starting from peptide-functionalized, aromatic dithiol **1**. Molecule **1** undergoes oxidation to form a small DCL consisting of cyclic disulfides in different oligomeric states. Macrocycle $\mathbf{1}_5$ self-stabilizes by forming short stacks of rings, shifting the exchange pool towards the formation of $\mathbf{1}_5$. Short stacks elongate, resulting in a supramolecular polymer with a fiber-like structure. b) Schematic representation of the stepwise hydrogelation process. Fast triggered gelation is achieved by adding dialdehyde crosslinkers to the fiber solution through acyl-hydrazone formation. For clarity, only crosslinking with a dialdehyde is depicted. Covalent crosslinking interconnects the fibers, creating a 3D network containing a large amount of water. c) Di- and trialdehydes used for crosslinking of $\mathbf{1}_5$ fibers for hydrogel formation: glutaraldehyde (**2**), aldehyde-PEG-aldehyde, MW 600 (**3**), terephthaldehyde (**4**), isophthaldehyde (**5**), quinolone-based dialdehyde (**6**), benzene - 1,3,5 - tricarboxaldehyde (**7**) and triazine-based trialdehyde (**8**). d) Hydrogel formation upon the addition of different crosslinkers. Vial inversion tests indicate the formation of hydrogels in the presence of di- and trialdehydes containing short and rigid spacer groups, such as **2**, **4**, **5**, and **7**.

between carbonyl groups and spacer flexibility enables hydrazone formation within a single fiber.

To probe how gel formation depends on the concentration of **1**, we prepared a series of samples at building block concentrations ranging from 4.0 mM to 0.25 mM, while using glutaraldehyde (**2**) as a model crosslinker. Remarkably, the critical gelation concentration (CGC) was found to be 0.5 mM (in **1**), corresponding to 0.025 wt % (Figure S27), which is at the low end of the scale for hydrogels reported in the literature.[22] At 0.25 mM, the sample exists as a viscous solution. Similar observations were made using terephthalaldehyde (**4**) as a crosslinking agent (Figure S28).

To directly visualize the organization of fibers in the hydrogels, we used cryo-TEM. The appearances of the samples with and without crosslinkers (Figure S29) are remarkably similar, despite the distinct differences in viscosity. Regardless of the crosslinker, the samples do not exhibit longer-range order within the hydrogel network.

The mechanical properties of the hydrogels were evaluated using rheology, in which the storage (or elastic) modulus G′ and the loss (or viscous) modulus G″ were characterized. In frequency sweeps (0.1–100 rad/s), G′ always dominates G″, and both G′ and G″ are nearly independent on frequency for all crosslinkers (Figure 1a). This feature was also observed in previous studies on fibrillar hydrogels and suggests that the disentanglement is sufficiently slow that it occurs outside the tested frequency range.[23]

To investigate the fracture resistance of the materials, strain sweeps were performed for a wide range of $\gamma = 0.01$–200 %, at $\omega = 1$ rad/s. Gel fracture occurs at almost the same strain in all samples, regardless of their G′ value (Figure 1b). Such behavior is consistent with fiber strength (not crosslinking) being the common denominator for all hydrogels. By applying strain, the stacks of macrocycles are broken, rather than the covalent bonds that are responsible for crosslinking. Interestingly, strain-hardening before the failure is observed with hydrogels crosslinked by aldehydes with two functional groups and much less with compound **7**, which has three carbonyl groups. This suggests that strain hardening is connected to fiber network topology under shear,[24] while cryo-TEM of static samples shows no difference among the different networks at a length scale of 250 nm (Figure S29). Finally, after the strain sweep-induced fracture, the hydrogels partially recovered within the time they were monitored. It is clear that the recovery rate for all samples is much slower than the gelation rate, as indicated in Figure 1c. Perhaps counterintuitively, in this system covalent hydrazone bond formation is faster than non-covalent fiber re-assembly. AFM micrographs of the gel after the recovery process (Figure S34) indicate that the fibers are shorter than before the gel's fracture, consistent with the relatively low storage modulus (G′) attained upon slow healing.

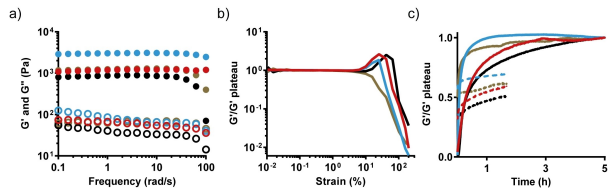

Figure 1. a) Frequency sweep: Storage modulus (full circles) and loss modulus (hollow circles) at $\gamma = 0.5$ % as a function of angular frequency for gels with different crosslinkers. b) Strain sweeps: Storage modulus versus amplitudes, at angular frequency $\omega = 1$ rad/s of gels with different crosslinkers, normalized by the G′ plateau value obtained prior to applying strain sweeps. c) Gelation (solid line) and recovery (dashed line): Storage moduli during formation and recovery processes as a function of time for gels with different crosslinkers, normalized by the G′ plateau value obtained prior to applying strain sweeps. Crosslinkers: **2** (red), **4** (blue), **5** (black), and **7** (gold). Detailed rheological data are shown in Figures S30–S33.

To exploit the dynamic behaviour of the acyl-hydrazone bond, we investigated the responsiveness of the hydrogels towards a chemical stimulus. Exploiting the greater stability of oximes compared to acyl hydrazones, we employed NH_2OH (**9**) as a chemical stimulus (Scheme S1). We prepared a 0.50 mL sample of hydrogel at 5.0 mM concentration (in **1**, 12.5 mM borate buffer, pH 8.2) in an NMR tube by introducing crosslinker **2** (Figure S35a–ii). In a separate layer on top of the gel, 0.10 mL of a solution of NH_2OH, equimolar with respect to the hydrazone moieties, was added (Figure S35a–iii). The NH_2OH solution was allowed to diffuse into the gel leading to its degradation (Figure S35a–iv). The degradation process took seven days to complete, most likely due to the low reactivity of acyl-hydrazones towards the N-nucleophiles under near-physiological conditions and slow diffusion through the gel. The reaction was followed by ^{1}H NMR spectroscopy. The condensation of **2** and NH_2OH is evident from the appearance of aldoxime proton signals of the *cis* and *trans* isomers of the oxime product (**10** in Scheme S1; see Figure S36). To confirm that the gel degradation does not arise from the degradation of fibers, we performed AFM imaging of the obtained solution. As shown in Figure S35b, fibers persist. A second solution to gel transition was achieved upon adding another portion of **2**, as revealed by inversion of the NMR tube (Figure S35a panel v).

Dynamic covalent chemistry is influenced by pH, and acyl-hydrazones are particularly known for hydrolysis in acidic environments ($pH \approx 4$–6).[25] In order to examine the stability of the hydrogels at different pHs, we exposed hydrogels prepared from $\mathbf{1_5}$ and **4** to solutions buffered at pH 4.5, 6.0 and 7.4. The hydrogels at pH 6 and 7.4 showed good stability over 17 days of exposure, but at pH 4.5 after 4 days the gel collapsed partially (Figure S37).

Having established that reversible covalent chemistry can be used for constructing fibers and their subsequent crosslinking, we probed their potential for covalent functionalization with RGD and LDV, as biologically relevant peptide motifs.[26] Supramolecular, self-assembled structure ($\mathbf{1_5}$) was obtained as previously established. After UPLC/MS analysis confirmed that the sample was dominated by $\mathbf{1_5}$ (Figure 2a), the preformed assembly was split into two and reacted with 10 mol % of **glyoxylyl-RGD** or **glyoxylyl-LDV**, respectively (Figure 2a). Upon stirring (30 min), UPLC-MS

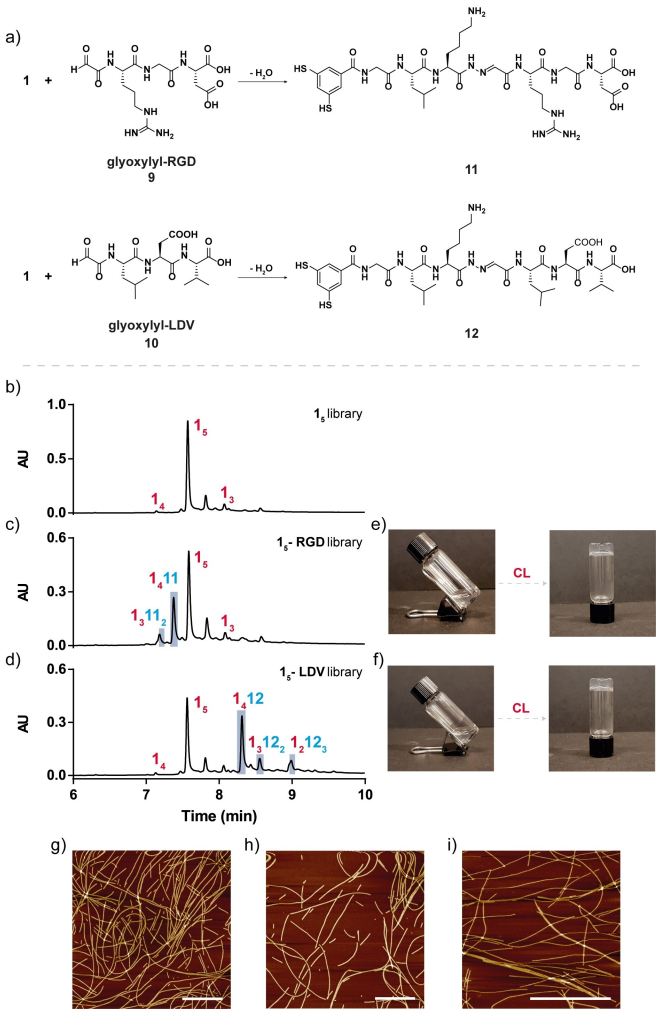

Figure 2. a) Structures of acyl hydrazone building blocks that form in situ upon reacting assemblies of $\mathbf{1}_5$ with aldehyde-functionalized RGD (**9**) or LDV (**10**) peptides. For clarity hydrazones **11** and **12** are shown as dithiols, even though they exist mostly as mixed disulfide oligomers in the experiments. b) UPLC analyses of DCLs made by oxidation and disulfide exchange of **1** (4.0 mM) in borate buffer (12.5 mM, pH 8.2) stirred at 1200 rpm: b) when dominated by self-assembly $\mathbf{1}_5$; c) after post-modification of $\mathbf{1}_5$ by **glyoxylyl-RGD** ($\mathbf{1}_5$**-RGD**) and d) **glyoxylyl-LDV** ($\mathbf{1}_5$**-LDV**), both recorded 30 min after addition of the corresponding aldehyde. Formed acyl-hydrazones (mixed species) are highlighted in blue. Hydrogel formation upon addition of crosslinker **4** to DCLs dominated by $\mathbf{1}_5$ and post-modified with e) **glyoxylyl-RGD** ($\mathbf{1}_5$**-RGD**) and f) **glyoxylyl-LDV** ($\mathbf{1}_5$**-LDV**). The vial inversion test indicates the formation of hydrogels within 2 minutes after the addition of crosslinker. Representative AFM images of DCLs g) dominated by $\mathbf{1}_5$; obtained after post-modification of $\mathbf{1}_5$ with h) **glyoxylyl-RGD** and i) **glyoxylyl-LDV**. Scale bars are equal to 500 nm.

analysis of the two samples showed successful covalent modification of $\mathbf{1}_5$ evident from the appearance of mixed self-assemblies ($\mathbf{1}_4(\mathbf{11})$, $\mathbf{1}_3(\mathbf{11})_2$, and $\mathbf{1}_4(\mathbf{12})$, $\mathbf{1}_3(\mathbf{12})_2$, $\mathbf{1}_2(\mathbf{12})_3$), while $\mathbf{1}_5$ also remained present (Figure 2c, d; Figure S14–S22). The reaction appears to be finished within 30 minutes, as a further change in library composition was not observed upon prolonged stirring (20 h; Figure S14, and Figure S18). Atomic force micrographs of the samples obtained after functionalization with the two tripeptides revealed the presence of fibers (Figure 2h, i), similar in appearance to the original sample of $\mathbf{1}_5$ (Figure 2g).

Given that most of the hydrazide groups in the tripeptide functionalized samples are still unreacted, we expected that it would still be possible to convert these samples into hydrogels upon addition of a crosslinker. Indeed, vial-inversion tests indicated efficient gel formation (within 2 minutes) upon addition of crosslinker **4** to fibers that were functionalized with **glyoxylyl-RGD** and **glyoxylyl-LDV** (Figure 2e, f).

The interactions of the resulting hydrogels crosslinked with dialdehyde **4** with cells were evaluated by assessing cell viability levels and morphology, as these parameters are good indicators of biocompatibility. To quantify the survival of cells, live/dead analysis was performed using fluorescence microscopy. Human bone marrow-derived mesenchymal stem cells (hBM-MSCs) were seeded on top of hydrogels made by crosslinking of $\mathbf{1}_5$, $\mathbf{1}_5$**-RGD** and $\mathbf{1}_5$**-LDV** libraries by adding dialdehyde **4**, followed by the incubation. After one day, the hydrogels with seeded cells were stained by two fluorescent dyes, calcein-AM (green, live cells) and propidium iodide (PI, red, dead cells) (for the protocol, see Supporting Information). The material showed a minimal negative effect on cell toxicity as nearly 100 % of the cells remained alive (Figure 3a, for quantification Figure 3b).

To determine the effect of the RGD and LDV sequences on the morphology of the hBM-MSCs, cells were cultured on the three types of substrates for one day. After that, cells were fluorescently labelled to visualize their nuclei (DAPI) and cytoskeleton (FITC-phalloidin), (Figure 4). From fluorescent imaging of the cytoskeleton, it was observed that hBM-MSCs exhibit extended morphologies on all three types of materials without significant differences between them. In an attempt to clarify the reason behind the absence of a clear influence of cell adhesion peptides on cell morphology, we analyzed the effect of serum in the medium on cell-matrix interactions for the unmodified and peptide-modified gels. Under serum-free conditions cells were found

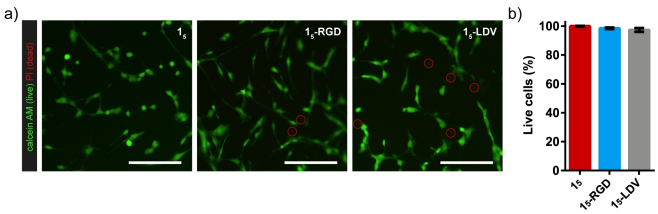

Figure 3. Representative fluorescence microscopy images of hBM-MSCs cultured on hydrogels made from $\mathbf{1}_5$ **fibers**, $\mathbf{1}_5$ **fibers** post-modified with **glyoxylyl-RGD**, and $\mathbf{1}_5$ **fibers** post-modified with **glyoxylyl-LDV**, and coated on glass coverslips in growth medium, stained with: a) calcein-AM (live cells; green) and propidium iodide (dead cells; red), after 24 h. For clarity, red circles emphasize the presence of dead cells and scale bars equal to 150 μm. b) Quantification of the viability of cells cultured on three different types of hydrogel-coated glass coverslips in growth medium for three repetitions of each type of material. Mean ± SD ($n = 3$, at least three random image fields per experiment, at least 50 counted cells per image field).

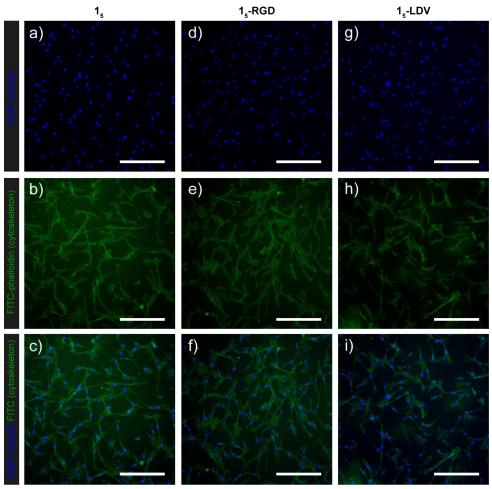

Figure 4. Representative fluorescence microscopy images of hBM-MSCs cells, cultured on hydrogels made from a)–c) **1_5 fibers**; d)–f) **1_5 fibers** post-modified with **glyoxal-RGD** and g)–j) **1_5 fibers** post-modified with **glyoxal-LDV**, stained with DAPI (blue) and FITC-phalloidin (cytoskeleton), after 24 h. The bottom images represent the merge of two channels. Scale bars equal to 300 μm.

to spread less efficiently for both types of gel (Figure S39), suggesting that serum proteins are promoting cell adhesion. However, the absence of difference in cell spreading between modified and unmodified hydrogels remains incompletely understood.

Conclusion

In summary, we designed a pseudo-peptide building block **1** capable of producing self-synthesizing nanofibers upon macrocyclization (producing $\mathbf{1}_5$) and supramolecular polymerization under mild aqueous conditions. These fibers display hydrazide groups on their surface, allowing for rapid and facile hydrogelation upon adding a crosslinker containing two or three aldehyde groups. Rheology measurements revealed that both storage and loss moduli of all hydrogels, regardless of the crosslinker used, are frequency independent, while high amounts of stress induce gel fracture. The hydrogels can be broken down through an exchange reaction with hydroxylamine and regenerated upon subsequent addition of crosslinker. Stability of the hydrogels at neutral and slightly acidic pH (pH ≈ 6) allows application for cell culture and tissue engineering (including application in tumors), and on the other hand, lability of the system at acidic pH opens up possibilities for drug delivery through endocytosis. The self-assembled fibers are readily functionalizable with RGD and LDV peptide sequences. Finally, the hydrogels formed by crosslinking of fibers of $\mathbf{1}_5$, as well as $\mathbf{1}_5$-**RGD** and $\mathbf{1}_5$-**LDV** showed to be biocompatible, manifested by the high viability of human bone marrow-derived mesenchymal stem cells when cultivated on these hydrogels. To our surprise, the cells adhered equally well to the native $\mathbf{1}_5$ and modified hydrogels, displaying elongated morphologies, characteristic of cell adhesion and spreading. Further studies are underway to exploit the potential of this modular material fully.

In conclusion, using a combination of two reversible covalent chemistries, we established a modular approach for the fabrication of tailor-made, molecularly engineered soft materials with considerable potential for use as a matrix for tissue culture. This new platform allows for facile and independent tuning of chemical and physical properties of the hydrogels.

Acknowledgements

We are grateful for the financial support from the Dutch Polymer Institute (DPI project 731.015.504), the Netherlands Organization for Scientific Research (NWO), the European Union (Marie Sklodowska-Curie grant 642192, MCIF 745805-DSR and ERC AdG 741774), the Dutch Ministry of Education, Culture and Science (gravitation program 024.001.035) and China Scholarship Council no. 201608310113.

Conflict of Interest

The authors declare no conflict of interest.

Data Availability Statement

The data that support the findings of this study are available from the corresponding author upon reasonable request.

Keywords: Cell Adhesion · Dynamic Covalent Chemistry · Hydrogels · Self-Assembly · Tailor-Made Materials

[1] a) H. Shin, S. Jo, A. G. Mikos, *Biomaterials* **2003**, *24*, 4353–4364; b) P. X. Ma, *Adv. Drug Delivery Rev.* **2008**, *60*, 184–198; c) J. Patterson, M. M. Martino, J. A. Hubbell, *Mater. Today* **2010**, *13*, 14–22.
[2] a) C. A. E. Hauser, S. Zhang, *Chem. Soc. Rev.* **2010**, *39*, 2780–2790; b) S. Zhang, *Nat. Biotechnol.* **2003**, *21*, 1171–1178.
[3] H. Cui, M. J. Webber, S. I. Stupp, *Biopolymers* **2010**, *94*, 1–18.
[4] a) O. J. G. M. Goor, S. I. Hendrikse, P. W. Dankers, E. W. Meijer, *Chem. Soc. Rev.* **2017**, *46*, 6621–6637; b) K. Sato, M. P. Hendricks, L. C. Palmer, S. I. Stupp, *Chem. Soc. Rev.* **2018**, *47*, 7539–7551.
[5] P. Y. W. Dankers, M. C. Hamsen, L. A. Brouwer, M. J. A. Van Luyn, E. W. Meijer, *Nat. Mater.* **2005**, *4*, 568–574.
[6] G. A. Silva, C. Czeisler, K. L. Niece, E. Beniash, D. A. Harrington, J. A. Kessler, S. I. Stupp, *Science* **2004**, *303*, 1352–1355.
[7] M. P. Lutolf, J. L. Lauer-Fields, H. G. Schmoekel, A. T. Metters, F. E. Weber, G. B. Fields, J. A. Hubbel, *Proc. Natl. Acad. Sci. USA* **2013**, *100*, 9413–9418.
[8] M. P. Lutolf, J. A. Hubbell, *Nat. Biotechnol.* **2005**, *23*, 47–55.
[9] P. Worthington, D. J. Pochan, S. A. Langhans, *Front. Oncol.* **2015**, *5*, 92.
[10] D. Seliktar, *Science* **2012**, *336*, 1124–1128.
[11] a) A. K. H. Hirsch, E. Buhler, J.-M. Lehn, *J. Am. Chem. Soc.* **2012**, *134*, 4177–4189; b) J.-M. Lehn, *Angew. Chem. Int. Ed.*

2015, *54*, 3276–3289; *Angew. Chem.* **2015**, *127*, 3326–3340; c) N. Roy, Bruchmann, J.-M. Lehn, *Chem. Soc. Rev.* **2015**, *44*, 3786–3807; d) N. Giuseppone, J.-M. Lehn, *Angew. Chem. Int. Ed.* **2006**, *45*, 4619–4624; *Angew. Chem.* **2006**, *118*, 4735–4740; e) L. Tauk, A. P. Schröder, G. Decher, N. Giuseppone, *Nat. Chem.* **2009**, *1*, 649–656; f) E. Lutz, E. Moulin, V. Tchaskalova, D. Benczédi, A. Herrmann, N. Giuseppone, *Chem. Eur. J.* **2021**, *27*, 13457–13467; g) J. W. Sadownik, R. V. Ulijn, *Chem. Commun.* **2010**, *46*, 3481–3483; h) C. Berdugo, S. K. Mohan Nalluri, N. Javid, B. Escuder, J. F. Miravet, R. V. Ulijn, *ACS Appl. Mater. Interfaces* **2015**, *7*, 25946–25954; i) C. G. Pappas, R. Shafi, I. R. Sasselli, H. Siccardi, T. Wang, V. Narang, R. Abzalimov, N. Wijerathne, R. V. Ulijn, *Nat. Nanotechnol.* **2016**, *11*, 960–967; j) J. Solà, M. Lafuente, J. Atcher, I. Alfonso, *Chem. Commun.* **2014**, *50*, 4564–4566; k) M. Lafuente, J. Solà, I. Alfonso, *Angew. Chem. Int. Ed.* **2018**, *57*, 8421–8424; *Angew. Chem.* **2018**, *130*, 8557–8560.

[12] a) J. M. A. Carnall, C. A. Waudby, A. M. Belenguer, M. C. A. Stuart, J. J.-P. Peyralans, S. Otto, *Science* **2010**, *327*, 1502–1506; b) M. Colomb-Delsuc, E. Mattia, J. W. Sadownik, S. Otto, *Nat. Commun.* **2015**, *6*, 7427–7433; c) Y. Altay, M. Tezcan, S. Otto, *J. Am. Chem. Soc.* **2017**, *139*, 13612–13615; d) J. W. Sadownik, D. Philp, *Angew. Chem. Int. Ed.* **2008**, *47*, 9965–9970; *Angew. Chem.* **2008**, *120*, 10113–10118; e) T. Kosikova, D. Philp, *J. Am. Chem. Soc.* **2019**, *141*, 3059–3072; f) B. Liu, C. G. Pappas, E. Zangrando, N. Demitri, P. J. Chmielewski, S. Otto, *J. Am. Chem. Soc.* **2019**, *141*, 1685–1689; g) C. G. Pappas, P. K. Mandal, B. Liu, B. Kauffmann, X. Miao, D. Komáromy, W. Hoffmann, C. Manz, R. Chang, K. Liu, K. Pagel, I. Huc, S. Otto, *Nat. Chem.* **2020**, *12*, 1180–1186.

[13] a) G. Deng, F. Li, H. Yu, F. Liu, C. Liu, W. Sun, H. Jiang, Y. Chen, *ACS Macro Lett.* **2012**, *1*, 275–279; b) L. He, D. Szopinski, Y. Wu, G. A. Luinstra, P. Theato, *ACS Macro Lett.* **2015**, *4*, 673–678.

[14] M. M. Perera, N. Ayers, *Polym. Chem.* **2020**, *11*, 1410–1423.

[15] a) A. G. Orrillo, A. M. Escalante, R. L. E. Furlan, *Chem. Commun.* **2008**, *42*, 5298–5300; b) A. G. Orrillo, A. La-Venia, A. M. Escalante, R. L. E. Furlan, *Chem. Eur. J.* **2018**, *24*, 3141–3146; c) A. G. Orrillo, A. M. Escalante, M. Martinez-Amezaga, I. Cabezudo, R. L. E. Furlan, *Chem. Eur. J.* **2019**, *25*, 1118–1127; d) N. Sakai, M. Lista, O. Kel, S. Sakurai, D. Emery, J. Mareda, E. Vauthey, S. Matile, *J. Am. Chem. Soc.* **2011**, *133*, 15224–15227; e) M. Lista, J. Areephong, N. Sakai, S. Matile, *J. Am. Chem. Soc.* **2011**, *133*, 15228–15230; f) N. Sakai, S. Matile, *J. Am. Chem. Soc.* **2011**, *133*, 18542–18545; g) E. Orentas, M. Lista, N.-T. Lin, N. Sakai, S. Matile, *Nat. Chem.* **2012**, *4*, 746–750; h) G. Sforazzini, R. Turdean, N. Sakai, S. Matile, *Chem. Sci.* **2013**, *4*, 1847–1851; i) C. Gehin, J. Montenegro, E.-K. Bang, A. Cajaraville, S. Takayama, H. Hirose, S. Futaki, S. Matile, H. Reizman, *J. Am. Chem. Soc.* **2013**, *135*, 9295–9298; j) M. J. Barrell, A. G. Campaña, M. von Delius, E. M. Geertsema, D. A. Leigh, *Angew. Chem. Int. Ed.* **2011**, *50*, 285–290; *Angew. Chem.* **2011**, *123*, 299–304.

[16] a) J. Chen, Q. Su, R. Guo, J. Zhang, A. Dong, C. Lin, J. Zhang, *Macromol. Chem. Phys.* **2017**, *218*, 1700166; b) J. Collins, M. Nadgorny, Z. Xiao, L. A. Connal, *Soft Matter* **2013**, *9*, 4635–4641.

[17] J. Kalia, R. T. Raines, *Curr. Org. Chem.* **2010**, *14*, 138–147.

[18] a) U. Hersel, C. Dahmen, H. Kessler, *Biomaterials* **2003**, *24*, 4385–4415; b) M. C. Cringoli, C. Romano, E. Parisi, L. J. Waddington, M. Melchionna, S. Semeraro, R. De Zorzi, M. Grönholm, S. Marchesan, *Chem. Commun.* **2020**, *56*, 3015–3018.

[19] R. Patel, M. Santosh, J. Kumar Dash, R. Karpoormath, A. Jha, J. Kwak, M. Patel, J. Hak Kim, *Polym. Adv. Technol.* **2019**, *30*, 4–12.

[20] a) A. N. Jonker, D. W. P. M. Löwik, J. C. M. van Hest, *Chem. Mater.* **2012**, *24*, 759–773; b) J. Li, R. Xing, S. Bai, X. Yan, *Soft Matter* **2019**, *15*, 1704–1715.

[21] a) A. Pal, M. Malakoutikhah, G. Leonetti, M. Tezcan, M. Colomb-Delsuc, V. D. Nguyen, J. van der Gucht, S. Otto, *Angew. Chem. Int. Ed.* **2015**, *54*, 7852–7856; *Angew. Chem.* **2015**, *127*, 7963–7967; b) M. Malakoutikhah, M. Colomb-Delsuc, H. Fanlo-Virgos, J. J.-P. Peyralans, M. C. A. Stuart, S. Otto, *J. Am. Chem. Soc.* **2013**, *135*, 18406–18417; c) P. Nowak, M. Colomb-Delsuc, S. Otto, J. Li, *J. Am. Chem. Soc.* **2015**, *137*, 10965–10969.

[22] X. Du, J. Zhou, J. Shi, B. Xu, *Chem. Rev.* **2015**, *115*, 13165–13307.

[23] V. D. Nguyen, A. Pal, F. Snijkers, M. Colomb-Delsuc, G. Leonetti, S. Otto, J. van der Gucht, *Soft Matter* **2016**, *12*, 432–440.

[24] C. Storm, J. J. Pastore, F. C. MacKintosh, T. C. Lubensky, P. A. Janmey, *Nature* **2005**, *435*, 191–194.

[25] S. Ulrich, *Acc. Chem. Res.* **2019**, *52*, 510–519.

[26] a) E. G. Hayman, M. D. Pierschbacher, Y. Ohgren, E. Ruoslahti, *Proc. Natl. Acad. Sci. USA* **1983**, *80*, 4003–4007; b) G. Feng, J. Zhang, Y. Li, Y. Nie, D. Zhu, R. Wang, J. Liu, J. Gao, N. Liu, N. He, W. Du, H. Tao, Y. Che, Y. Xu, D. Kong, Q. Zhao, Z. Li, *J. Am. Soc. Nephrol.* **2016**, *27*, 2357–2369; c) Y. Shi, D. S. Ferreira, J. Banerjee, A. R. Pickford, H. S. Azevedo, *Biomater. Sci.* **2019**, *7*, 5132–5142; d) P. Ung, D. A. Winkler, *J. Med. Chem.* **2011**, *54*, 1111–1125; e) K. Shiba, *Chem. Soc. Rev.* **2010**, *39*, 117–126; f) S. Caputi, O. Trubiani, B. Sinjari, S. Trofimova, F. Diomed, N. Linkova, A. Diatlova, V. Khavinson, *Int. J. Immunopathol. Pharmacol.* **2019**, *33*, https://doi.org/10.1177/2058738419828613.

Manuscript received: November 8, 2022
Accepted manuscript online: February 6, 2023
Version of record online: February 24, 2023